J. Fluid Mech. (1978), *vol.* 86, *part* 3, *pp.* 465–490
Printed in Great Britain

The uniform distortion of thermal and velocity mixing layers

By J. F. KEFFER, J. G. KAWALL,
Department of Mechanical Engineering, University of Toronto, Ontario, Canada
J. C. R. HUNT AND M. R. MAXEY
Department of Applied Mathematics and Theoretical Physics, University of Cambridge

(Received 13 January 1975 and in revised form 28 February 1976)

Two similar problems are considered: what is the effect of applying a uniform and constant rate of strain (i) to the two-dimensional thermal mixing region in a homogeneous grid-generated turbulent field, and (ii) to the two-dimensional velocity mixing region formed between two uniform streams moving with different mean velocities? The imposed strain field is orientated so as to compress or separate the isothermal and isokinetic surfaces in the plane of interest.

Two theoretical models are presented; in the first, the profiles of temperature and velocity are assumed to be self-preserving and an assumption is made about the velocity scales; in the second, the statistical, rapid-distortion approach to dispersion due to Hunt & Mulhearn (1973) is applied. The circumstances in which these models differ and those where the simpler self-preserving model can be applied are determined. The measurements presented here indicate that the widths of both mixing layers decrease within the strain field, the width of the thermal mixing layer decreasing at a greater rate than that of the velocity mixing layer. However, the measured length scales were found to be 5 % larger than the scales predicted by either of the analyses, which differed from each other by 5 %. It is suggested that selective amplification of the energy-containing eddies by the strain field is responsible.

1. Introduction

The application of a gross uniform strain to a turbulent flow is a problem of fundamental interest. As a diagnostic device it can often reveal important aspects of the structure of the motion. For example, the investigations of Townsend (1954), Tucker & Reynolds (1968) and Maréchal (1972) on uniform and constant straining of homogeneous turbulence have shed some light on the equilibrium structure which can be attained by a strained turbulent field, although the interpretations of the results are somewhat conflicting. In another flow situation, the experiments of Reynolds (1962) and Keffer (1965, 1967) on a two-dimensional wake have shown that some of the large entraining eddies in the outer regions of the flow may be amplified by a properly orientated strain field with the result that advection of quantities, such as turbulent energy, by a bulk convection mechanism is enhanced.

The examination of strain applied to a contaminant field has received comparatively little attention. In an early paper, Mills & Corrsin (1959) studied the effect of a

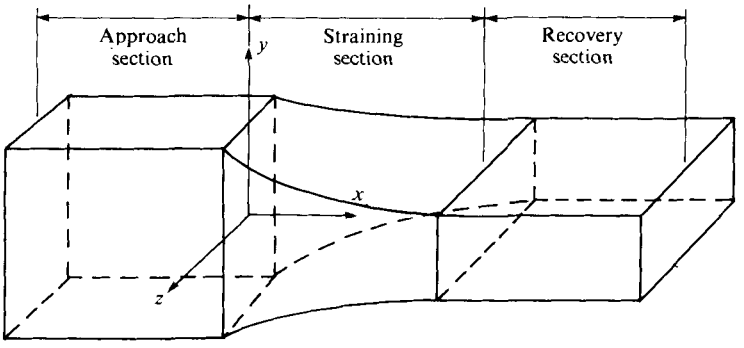

FIGURE 1. Schematic diagram of wind tunnel.

contraction upon velocity and temperature fluctuations in a homogeneous turbulent flow generated by a warm grid. They found that the anisotropy in the temperature field resulted in an increase in the smearing or dissipation of the thermal fluctuations.

In the first investigation reported here we examine a more complex motion: the effect of a suddenly imposed, uniform rate of strain upon a contaminant mixing layer which is generated by a step change in temperature in a homogeneous turbulent flow. At sufficiently low levels of heat input, the buoyancy forces are small enough that the temperature can be considered a passive scalar quantity.

In the second investigation, we measure the effect of a strain field on the thickness of the turbulent shear layer between two uniform streams with low but significant turbulence levels. The details of the turbulence in the shear layers are not measured. It is found that the hypothesis of a self-preserving layer and an assumption about the velocity scale adequately describe the overall properties of the shear layer.

Our first investigation is an example of turbulent diffusion in a uniformly distorted flow field. When changes occur 'rapidly', i.e. in a time small compared with the Lagrangian time scale (or eddy 'turnover' time), a statistical theory for diffusion can be developed. We compare the new experimental results presented here with two theories, the first of which is based on the assumptions of a self-preserving form for the temperature in the mixing layer and constancy of the velocity scales in the layer, the second being the rapid-distortion theory for the turbulence allied to the diffusion theory of Hunt & Mulhearn (1973). This rather more complicated second theory shows that the self-preserving assumptions should be approximately valid, as indeed they are found to be.

These flows are not only of intrinsic interest but can have a bearing on practical problems of turbulent dispersion of pollutants in the vicinity of obstacles (hills and buildings), inasmuch as the presence of an obstacle in an otherwise undisturbed flow field causes distortion of the flow field (Hunt 1973; Britter, Hunt & Puttock 1976).

2. Experimental considerations

The wind tunnel used in this experiment has been fully described elsewhere (Portfors 1969). It is shown schematically in figure 1. It consists of an approach section $0{\cdot}46 \times 0{\cdot}23$ m by 1·5 m long, a straining section (or distortion duct) 0·75 m long and a

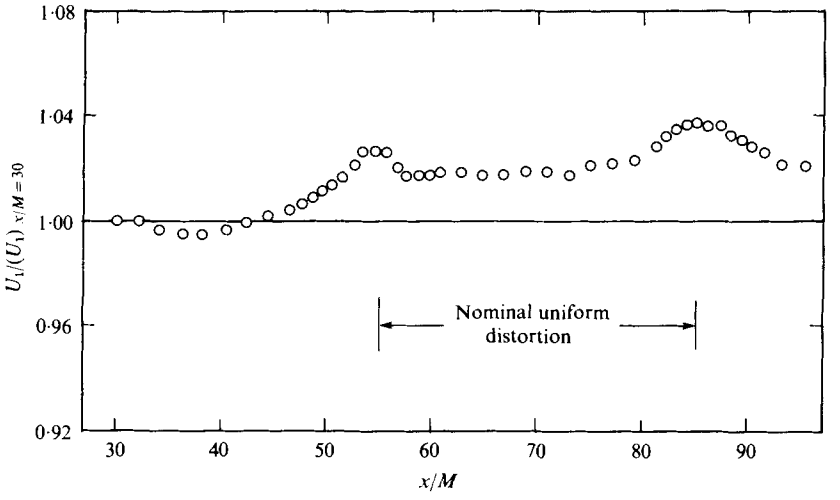

FIGURE 2. Variation of mean velocity along tunnel axis.

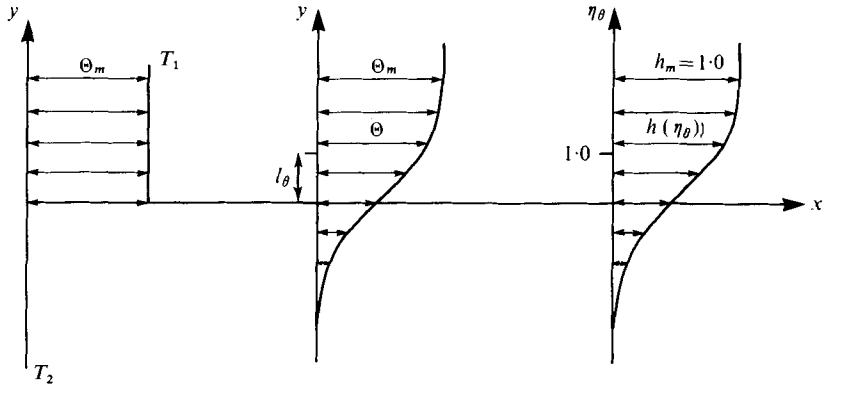

FIGURE 3. Definition sketch for temperature mixing layers.

recovery section 0·23 × 0·46 m by 0·75 m long. The cross-section dimensions are nominal as allowance was made for boundary-layer growth. The distortion duct is of constant cross-sectional area, the positions of the walls varying exponentially as

$$y = y_c \exp[-a(x-x_c)] = y_c\beta, \tag{2.1a}$$

$$z = z_c \exp[a(x-x_c)] = z_c\beta^{-1}, \tag{2.1b}$$

where the subscript c refers to conditions at the beginning of the distortion duct. The strain ratio is 2:1 for this duct (i.e. the maximum value of β^{-1} is 2·0), half that for the original duct of Townsend (1954) and much less than those for the McGill (Tucker & Reynolds 1968) and Grenoble (Maréchal 1972) ducts, which have strain ratios of 6:1 and 13·3:1, respectively. The resulting mean velocity field is

$$U = U_1 = \text{constant}, \quad V = -ayU_1, \quad W = azU_1, \tag{2.2a–c}$$

Source and type of grid	Present, parallel round rods	Comte-Bellot & Corrsin (1971), biplane, square rods	Van Atta & Chen (1969), biplane, round rods	Grant & Nisbet (1957), biplane, round rods
U_1 (ms^{-1})	6·1	10·0	15·7	6·3
M (mm)	25·4	25·4	25·4	50·8
Rod diameter, d (mm)	6·6	—	4·77	9·53
$R_M = U_1 M/\nu$	10,300	17,000	25,600	21,300
x/M	40	45	48	30
$\overline{(u^2)}^{\frac{1}{2}}/U_1$	0·0202	0·0205	0·0161	0·0212
$(\overline{u^2}/\overline{v^2})^{\frac{1}{2}}$	1·080	~ 0·976	1·130	1·132
$(\overline{u^2}/\overline{w^2})^{\frac{1}{2}}$	1·070	0·976	—	—
Longitudinal microscale, λ_u (mm)	6·40	—	—	—
Transverse microscale, λ_v (mm)	4·56	3·55	3·04	—
Transverse microscale, λ_w (mm)	4·63	—	—	—
Longitudinal integral scale, L_u (mm)	15·68	—	—	—
Transverse integral scale, L_v (mm)	6·46	6·00	—	—
Transverse integral scale, L_w (mm)	6·42	—	—	—
Dissipation rate, ϵ (m^2 s^{-3})	0·165	0·754	1·240	—
Kolmogorov scale, η (mm)	0·380	0·260	0·230	—
$R_\lambda = \overline{(u^2)}^{\frac{1}{2}} \lambda_v/\nu$	37·40	48·60	49·40	—

TABLE 1. Grid-flow properties.

where the constant a is 0·9094 m^{-1}. The mean velocities and turbulent intensities within the tunnel were checked experimentally using a Pitot–static tube in conjunction with a micromanometer and a constant-temperature hot-wire anemometer, respectively. It was found that the velocity field was satisfactorily uniform with the exception of slight streamwise accelerations of the mean flow in the vicinity of the start and end of the distortion duct (figure 2).

The step change in temperature was generated by electrically heating the upper half of a grid of parallel rods mounted in the wind tunnel to a uniform temperature and keeping the lower half of the grid at room temperature. The grid was constructed of 6·6 mm diameter heating rods, with their centres 25·4 mm apart (mesh length M = 25·4 mm), and was located 55 mesh lengths upstream of the entrance to the distortion duct. The turbulent field produced by the grid rapidly diffused the initial step profile into the developed flow (figure 3) which was subsequently subjected to the uniform strain field. The mean velocity U_1 of the background flow was 6·1 ms^{-1} and the maximum mean temperature difference $T_1 - T_2$ across the flow was 8 °C. As Keffer, Olsen & Kawall (1977) point out, the buoyancy force resulting from the temperature difference across a thermal mixing layer will have a negligible effect on the dynamics of the flow if the ratio of the Grashof number to the square

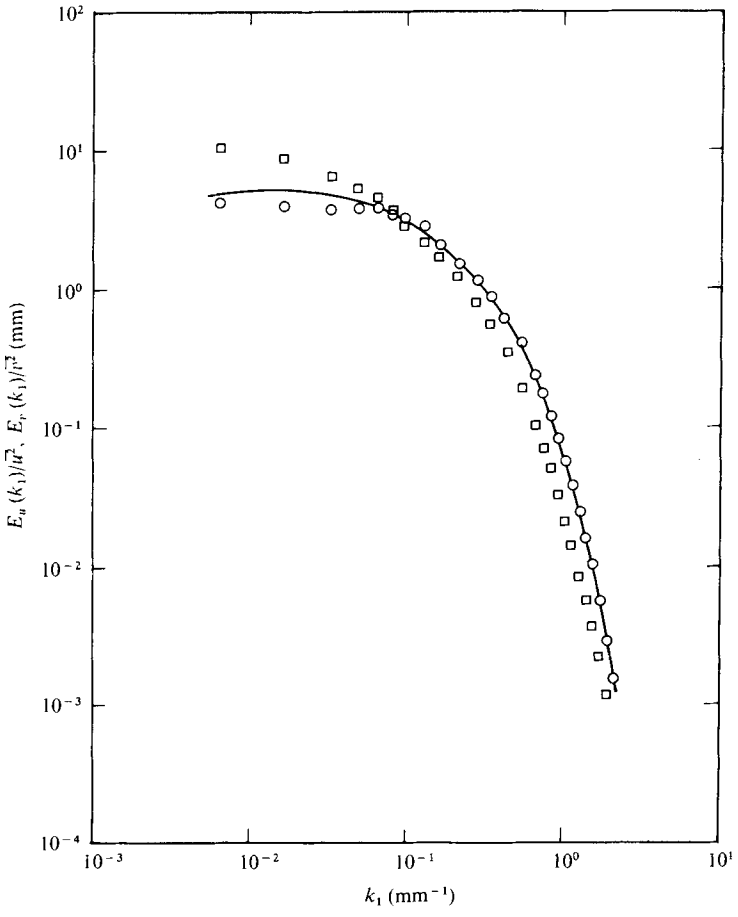

FIGURE 4. Normalized one-dimensional energy spectra of u^2 and v^2. □, E_u; ○, E_v; ——, E_v calculated from E_u using isotropic relation.

of the Reynolds number (which represents the ratio of the buoyancy force to the inertial force) is very much less than unity. In our present experiments, this ratio was of the order of 0·002. Thus the temperature field could be regarded as passive.

Characteristics of the background grid flow at $x/M = 40$ are reported in table 1. These were determined by means of constant-temperature hot-wire anemometry in conjunction with digital data processing. For comparison, grid-flow properties obtained by a number of other investigators are also given in table 1. It should be mentioned that the correlation coefficients

$$\overline{uv}/\overline{u^2}, \quad \overline{uw}/u^2, \overline{\left(\frac{\partial u}{\partial x}\right)\left(\frac{\partial v}{\partial x}\right)}\Big/\overline{\left(\frac{\partial u}{\partial x}\right)^2}, \quad \overline{\left(\frac{\partial u}{\partial x}\right)\left(\frac{\partial w}{\partial x}\right)}\Big/\overline{\left(\frac{\partial u}{\partial x}\right)^2}$$

were found to be essentially zero (less than 1 %) along the centre-line of the tunnel, as they should be, for reasons of symmetry. Figures 4, 5 and 6 show the one-dimensional spectra $E_u(k_1)$, $E_v(k_1)$ and $E_w(k_1)$ of the longitudinal and transverse components

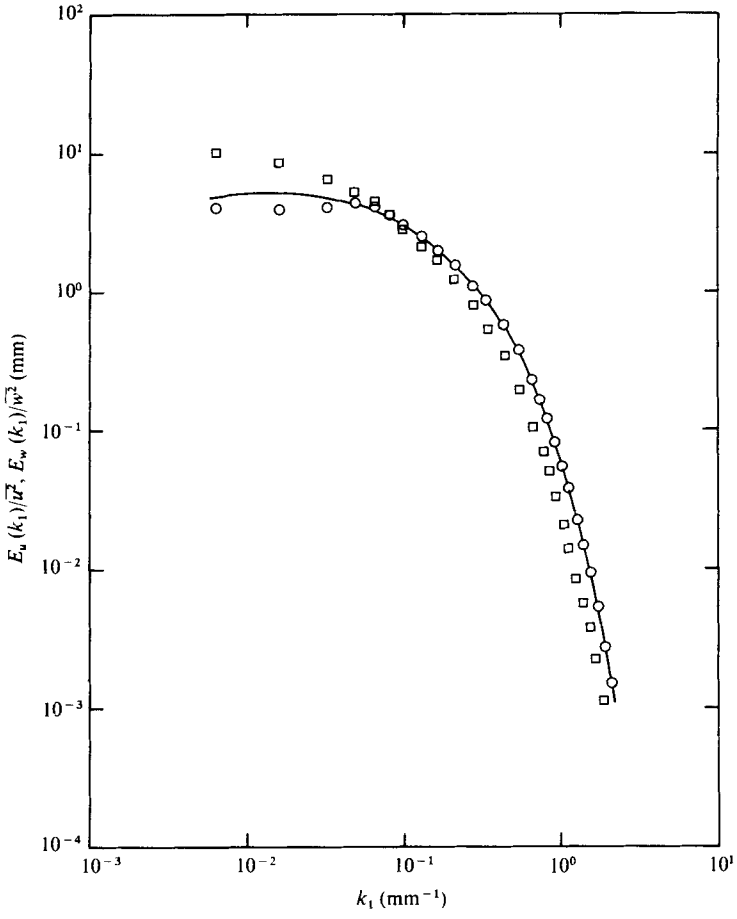

FIGURE 5. Normalized one-dimensional energy spectra of u^2 and w^2. □, E_u; ○, E_w; ——, E_w calculated from E_u using isotropic relation.

$\overline{u^2}$, $\overline{v^2}$ and $\overline{w^2}$ of the turbulent energy at $x/M = 40$, together with values of $E_v(k_1)$ and $E_w(k_1)$ calculated from $E_u(k_1)$ using the isotropic relation

$$E_{v,w} = \tfrac{1}{2}E_u[1 - \partial(\ln E_u)/\partial(\ln k_1)].$$

It is evident from these figures that the grid turbulence was approximately isotropic for wavenumbers greater than about 0·05 mm^{-1}, the departure from isotropy becoming more pronounced as the wavenumber approached zero. Thus it is not surprising that the ratio of the longitudinal integral scale to the transverse integral scale deviated from 2·0 (see table 1), the value necessary for complete isotropy, as the integral scales are strongly dependent on the low wavenumber structure of the turbulence (i.e. the large eddies). We note that the agreement between our measured and calculated E_v spectra is roughly the same as that found by Van Atta & Chen (1969) over the same wavenumber range ($\sim 0{\cdot}05$ mm$^{-1} \leqslant k_1 \leqslant \sim 2{\cdot}0$ mm^{-1}).

The velocity mixing layer was created by placing a fine mesh screen over the lower half of the unheated grid. No splitter plate was used. Nevertheless a step change in velocity was generated and the intense shear at the surface of discontinuity caused

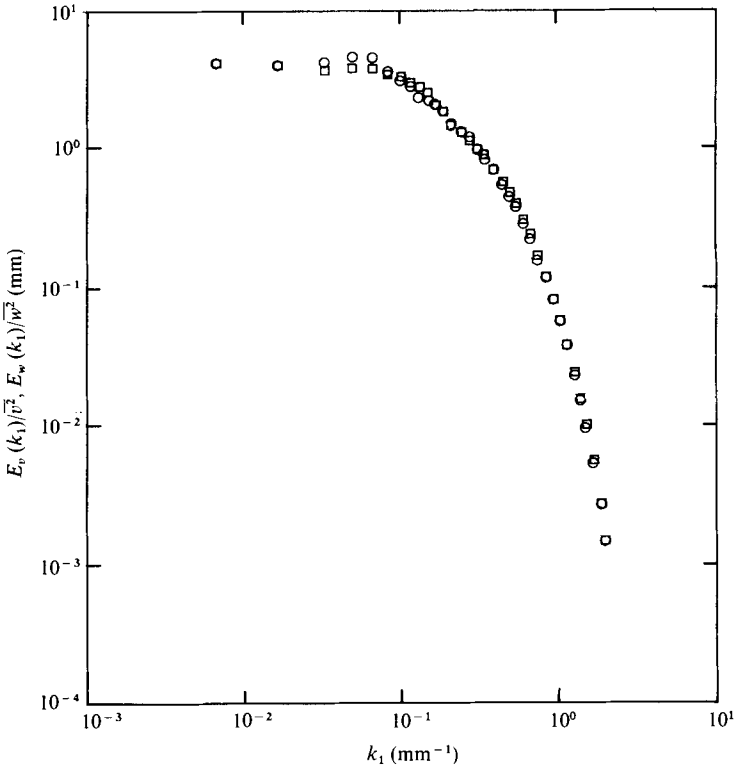

FIGURE 6. Normalized one-dimensional energy spectra of v^2 and w^2. □, E_v; ○, E_w.

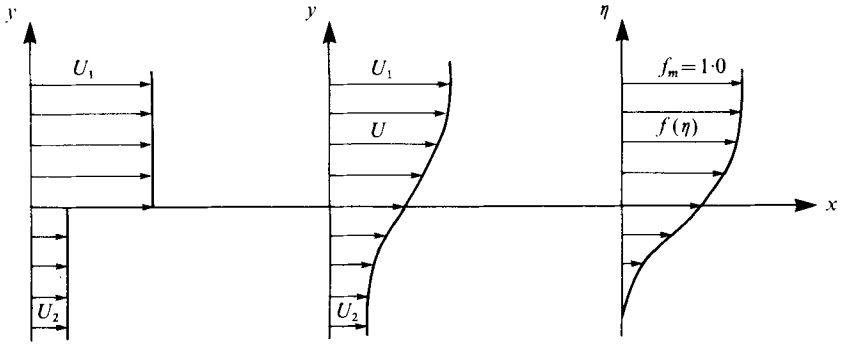

Initial profile Developed profile Dimensionless representation

FIGURE 7. Definition sketch for velocity mixing layer.

rapid subsequent diffusion.† Hence the flow profile quickly evolved into the developed mixing layer (figure 7). This was then subjected to a uniform strain field. The velocity of the upper stream was $U_1 = 7{\cdot}6$ ms^{-1} and that of the lower stream $U_2 = 4{\cdot}3$ ms^{-1}.

† It may be conjectured that, as the strength of the turbulence outside the shear layer was such that $\overline{(u^2)}^{\frac{1}{2}}/(U_1 - U_2) \doteq 0{\cdot}045$, the coherence of the large structures in the mixing (or shear) layer was probably reduced quite significantly.

The spreading of the mixing layers was studied as they developed in the streamwise direction. Measurements of mean temperatures and velocities were made in the pre-strain and post-strain sections of the tunnel as well as in the distortion duct. Temperature levels were determined by means of a copper–constantan thermocouple and velocities by means of a Pitot–static tube in conjunction with a micromanometer.

3. Analysis of the flow

Velocity mixing layer

The transverse spreading of unstrained mixing layers will be governed by the background turbulence and the mean shear. In the case of uniformly strained flows, the spreading will also be governed by the imposed strain field, which, because of its orientation with respect to the flows (i.e. streamlines converging in the x, y plane), should tend to inhibit the spreading. If sufficient development of a shear flow has taken place,† the distribution of mean flow quantities will be self-similar and characteristic intensity and length scales can be determined from these distributions to collapse the data. Also, the functional dependence of the scales upon the streamwise co-ordinate can be predicted from a self-preserving analysis based on the equations of mean motion. However, the solutions contain arbitrary constants, and although these can sometimes (as in wakes) be determined by integral constraints this cannot be done in this case.

Townsend (1976) has shown that the self-preserving intensity and length scales for a simple (i.e. undistorted) velocity mixing layer are given respectively by

$$u_0 = \text{constant}, \quad l_0 = C(x - x_0), \tag{3.1), (3.2}$$

where u_0 can be taken as the velocity difference $U_1 - U_2$ between the undisturbed adjacent streams, l_0 is proportional to the width of the layer, C is a constant and x_0 is some suitable virtual origin for the flow. C and x_0 are obtained from experiments. The turbulence adjusts itself to the local values of u_0 and l_0; so $(\overline{u^2})^{\frac{1}{2}}$ is proportional to u_0 and L_x, the Lagrangian integral scale, is proportional to l_0.

We assume that u_0 is approximately constant even in the distortion; then the analysis in appendix A shows that the length scale is given by

$$l_0/M = C \exp(-a^* r_1^2/2r_0)\left[\left(\frac{2r_0}{a^*}\right)^{\frac{1}{2}} \int_0^{r_1 a^{*\frac{1}{2}}/(2r_0)} \exp(t^2)\, dt + \frac{(x_1 - x_0)}{M}\right] \tag{3.3}$$

for $x_1 \leqslant x \leqslant x_2$ (non-uniform straining) and by

$$l_0/M = (C/a^*)\left[(a^* C_0 - 1)\exp(-a^* r_2) + 1{\cdot}0\right] \tag{3.4}$$

for $x \geqslant x_2$ (in the uniform-straining section), where $r_0 = (x_2 - x_1)/M$, $r_1 = (x - x_1)/M$, $r_2 = (x - x_2)/M$ and $a^* = aM$. The constant C_0 is given in terms of C by

$$C_0 = \exp(-\tfrac{1}{2}a^* r_0)\left[\left(\frac{2r_0}{a^*}\right)^{\frac{1}{2}} \int_0^{(\frac{1}{2}a^* r_0)^{\frac{1}{2}}} \exp(t^2)\, dt + \frac{x_1 - x_0}{M}\right].$$

† This implies that the flow is developing over a time scale *large* compared with the Lagrangian time scale $\tau_l \sim L_x/(\overline{u^2})^{\frac{1}{2}} \sim l_0/(\overline{u^2})^{\frac{1}{2}}$. The essential principle of self-preserving flows is that the conditions at the initiation of the flow are *largely irrelevant* and that the flow is governed by a moving equilibrium (Townsend 1976, p. 196).

Thermal mixing layer

Now consider the growth of a thermal mixing layer placed in a turbulent flow characterized by a local turbulent velocity u_1' and an integral scale L_x (see figure 3). The turbulence is not related to the dimensions of the mixing layer; it decays and is distorted by the duct quite independently of the mixing layer. Therefore it is not evident at first that a self-preserving solution is appropriate. However, for the same reason that the temperature downstream of a heated wire in a turbulent flow exhibits a self-similar profile, we expect that in a *uniform* turbulent flow the temperature profile in the mixing layer will be self-similar. When $x \ll L_x(\overline{U}/u_1')$ (i.e. travel times small compared with the Lagrangian or eddy time scale) the explanation for the self-similarity is based on the normality of the joint probability distributions for the turbulent velocities (Batchelor & Townsend 1956).

In the analysis described in appendix A we advance the two hypotheses that, even in turbulent flow where u_1' and L_x vary along the streamwise direction, (i) the temperature profiles remain self-similar and (ii) the variations in u_1' and L_x have insignificant effects compared with the straining of the mean flow by the contraction, if the straining is sufficiently strong. In other words the convergence of the mean streamlines dominates the dispersion. On the basis of these hypotheses we deduce expressions for the thickness l_θ of the thermal mixing layer, in the two distinct sections of the flow. In the pre-distortion section, l_θ increases linearly, i.e.

$$l_\theta = K(x - x_{\theta 0}), \tag{3.5a}$$

$x_{\theta 0}$ being a virtual origin for the thermal layer and K being a constant. As the flow enters the converging section, the slight non-uniform distortion in the region $x_1 \leqslant x \leqslant x_2$ produces a change in l_θ given by

$$l_\theta/M = K \exp(-a^* r_1^2/2r_0)\left[\left(\frac{2r_0}{a^*}\right)^{\frac{1}{2}} \int_0^{r_1(a^*/2r_0)^{\frac{1}{2}}} \exp(t^2)\,dt + \frac{x_1 - x_{\theta 0}}{M}\right], \tag{3.5b}$$

and in the uniform-distortion section ($x > x_2$),

$$l_\theta/M = (K/a^*)[(a^* K_0 - 1)\exp(-a^* r_2) + 1{\cdot}0], \tag{3.6a}$$

where

$$K_0 = \exp[-\tfrac{1}{2}(a^* r_0)]\left[\left(\frac{2r_0}{a^*}\right)^{\frac{1}{2}} \int_0^{(\frac{1}{2}a^* r_0)^{\frac{1}{2}}} \exp(t^2)\,dt + \frac{x_1 - x_{\theta 0}}{M}\right]. \tag{3.6b}$$

K is a constant which is fixed by comparison with the experimental results in the pre-strain section.

Note that the mixing-layer thicknesses l_0 and l_θ increase linearly in the pre-strain region, in the first case owing to the self-generated turbulence of the shear layer and in the second case owing to the uniform turbulence across the thermal layer. In the converging section both l_0 and l_θ decrease; the converging streamlines reduce the spreading of the two mixing layers. The theory does not indicate how strong the contraction must be for the natural growth of l_0 and l_θ due to the turbulence to be reversed by this mean-streamline effect. However a more complicated statistical theory, based on rapid-distortion ideas, can answer this question.

The development of the thermal mixing layer may be analysed in terms of the turbulent diffusion theory of Hunt & Mulhearn (1973). This theory calculates the

diffusive spread for a point source in terms of the Lagrangian velocity correlations; and these are in turn found from the theory of homogeneous rapid distortion of Batchelor & Proudman (1954). Suppose that the diffusive spread for a point source at the grid is $\sigma(x)$ in the y direction, so that $\sigma^2(x)$ is the variance of the plume width. Since the turbulence probability distribution in a homogeneous flow is approximately Gaussian it is reasonable to assume that the concentration of contaminant from a point source is normally distributed, and so in a vertical plane Oxy along the centre of the wind tunnel the temperature due to a point source is

$$T = [T_0/(2\pi\sigma^2(x))^{\frac{1}{2}}]\exp(-(y-Y)/2\sigma^2(x)). \tag{3.7}$$

The plume described above is centred on $y = Y(x)$ and Y depends on the convection by the mean flow, with $y = Y(0)$ initially. When $x \ll L_x\overline{u}/u_1'$, $\sigma(x) = [\overline{(v^2)}^{\frac{1}{2}}/\overline{u}]x$ (Monin & Yaglom 1971, chap. 5), and the heated grid may then be regarded as a superposition of independent point sources with

$$T = \begin{cases} T_0, & y > 0 \\ 0, & y < 0 \end{cases} \quad \text{at} \quad x = 0. \tag{3.8}$$

This leads to an overall temperature profile $T(x, y)$ given by

$$\begin{aligned} T(x,y) &= \int_0^\infty [Q(x)/(2\pi\sigma^2(x))^{\frac{1}{2}}]\exp[-(y-Y)^2/(2\sigma^2(x))]\,dY \\ &= \frac{Q(x)}{[2\pi\sigma^2(x)]^{\frac{1}{2}}}\int_{-y}^\infty \exp(-\eta^2/2\sigma^2(x))\,d\eta, \end{aligned} \tag{3.9}$$

where $Q(x)$ is a weighted source distribution allowing for the convergence of streamlines in the straining section. Thus the temperature profile should be given by the error function. It also follows that, for the definition of the mixing-layer thickness given in appendix A,

$$l_\theta = 2{\cdot}56\sigma(x).$$

Hence a knowledge of the diffusion of a point source will give the behaviour of l_θ as well. One feature of this statistical result is that the temperature profile is *self-similar*, even though the turbulence is not in equilibrium. The cause is the Gaussian nature of the turbulent velocity.

The result for l_θ is not altered if the centre of the straining motion and the centre of the mixing layer do not coincide. Also, if there is any three-dimensional structure with variation in the z direction this will only produce a scaling factor in the temperature profile without altering l_θ.

Consider now the motion of a single particle released into the turbulent flow prior to the initiation of the strain and in particular the y co-ordinate of its position. For a particle at $\mathbf{x} = \mathbf{X}\langle t\rangle$

$$\frac{dY}{dt} = V(\mathbf{X}\langle t\rangle, t) + v(\mathbf{X}\langle t\rangle, t), \tag{3.10}$$

where $v(\mathbf{x}, t)$ is the Eulerian velocity fluctuation. The mean velocity given in (2.2) shows that the mean velocity *normal* to the mean streamline through the source in the Oxy plane is

$$V = -a\langle t\rangle yU_1. \tag{3.11}$$

Hence

$$dY/dt = -a\langle t\rangle\, YU_1 + v(\mathbf{X}\langle t\rangle, t). \tag{3.12}$$

Following Hunt & Mulhearn (1973), the fluctuating velocity component is expanded as a Taylor series about its value at $\overline{\mathbf{X}}\langle t\rangle$, where $\overline{\mathbf{X}}\langle t\rangle$ is the mean position of the particle at time t on the mean streamline through the source:

$$dY/dt = -a\langle t\rangle\, YU_1 + v(\overline{\mathbf{X}}\langle t\rangle, t) + O[(X_i - \bar{X}_i)\,\partial v/\partial x_i|_{\overline{X}\langle t\rangle, t}]. \tag{3.13}$$

The last term of this equation may be estimated in terms of the turbulence as

$$O(l_\theta\, u_1'/L_x),$$

where l_θ is a scale of the diffusive spread, u_1' a scale of turbulent velocity fluctuation and L_x the longitudinal integral length scale. This term is negligibly small if, within the straining section, the following sufficient conditions are satisfied:

$$u_1'/(aU_1 L_x)(\simeq t/\tau_L) \ll 1, \quad l_\theta/L_x \ll 1,$$

where $\tau_L = L_x/u_1'$ is the Lagrangian time scale of the turbulence. These conditions indicate that diffusive spread must be small compared with the integral scale and that the theory applies to the initial stages of diffusion where the statistics of the particle motion are still well correlated. The first condition is also the requirement for the rapid-distortion theory of Batchelor & Proudman (1954) to be applicable.

The equation for dY/dt may be averaged:

$$d\overline{Y}/dt = -a\langle t\rangle U_1\, \overline{Y} + O(l_\theta\, u_1'/L_x), \tag{3.14}$$

which has the solution

$$\overline{Y}\langle t\rangle = \overline{Y}\langle 0\rangle \exp(-A\langle t\rangle U_1),$$

where

$$A\langle t\rangle = \int_{t_1}^{t} a\langle \tau\rangle\, d\tau = S(x)/U_1 \quad (x = U_1 t) \tag{3.15}$$

and t_1 is the instant at which the strain is initiated.

Similarly,

$$\bar{X}\langle t\rangle = U_1 t, \quad \bar{Z}\langle t\rangle = \bar{Z}(0)\exp(-A\langle \tau\rangle U_1).$$

If $v\langle t\rangle$ is defined as $v\langle t\rangle = v(\overline{\mathbf{X}}\langle t\rangle, t)$ then the equation for $Y - \overline{Y}$ is

$$d(Y - \overline{Y}\langle t\rangle)/dt = -a\langle t\rangle U_1 (Y - \overline{Y})\langle t\rangle + v\langle t\rangle, \tag{3.16}\dagger$$

which has the solution

$$Y - \overline{Y}\langle t\rangle = \exp(-A\langle t\rangle U_1) \int_0^t d\tau\, [\exp(A\langle \tau\rangle U_1)\, v\langle \tau\rangle], \tag{3.17}$$

so that

$$\overline{(Y\langle t\rangle - \overline{Y}\langle t\rangle)^2} \equiv \sigma^2 = \exp(-2A\langle t\rangle U_1) \times \int_0^t d\tau' \int_0^t d\tau''\, [\exp(A\langle \tau'\rangle U_1 + A\langle \tau''\rangle U_1)\, \overline{v\langle \tau'\rangle\, v\langle \tau''\rangle}]. \tag{3.18a}$$

† Note that this is formally identical to equations (A 6) and (A 17), in appendix A, which have been obtained by the self-preserving theory.

In the pre-strain turbulence this reduces to

$$\sigma^2 = \int_0^t d\tau' \int_0^t d\tau'' \overline{v\langle\tau'\rangle v\langle t''\rangle}. \tag{3.18b}$$

As $\bar{X}\langle t\rangle = U_1 t$, σ may equivalently be regarded as a function of time or of position downstream in the wind tunnel. The exponential factors in the integral for σ represent the effect of mean-streamline convergence in the y direction, produced in the straining section, and show how this convergence slows down the rate of diffusive spread or even reduces the plume width despite the turbulence. The Lagrangian autocorrelations $\overline{v\langle t_1\rangle v\langle t_2\rangle}$ are found from rapid-distortion theory, and the details are given in appendix B. It also follows from the result for $\bar{Y}\langle t\rangle$ that the weighting function $Q(x)$, defined in (3.9), is

$$Q(x) = \exp\left(A(t)\,U_1\right), \quad \text{where} \quad t = x/U_1.$$

The theory can show what happens if the straining is *large* and *negative*. This means that the streamlines diverge and that $a < 0$ and $|a|\, l_{\theta 1} U_1/u' = \Sigma \gg 1$, where $l_{\theta 1}$ is the value of l_θ at the beginning of the distortion, where $x = x_1$ and $t = t_1$. Then in (3.16) the term due to the divergence of the streamlines dominates and we find that as $\Sigma \to \infty$

$$Y - \bar{Y} \sim (Y - \bar{Y})(x = x_1) \exp\left(-U_1 \int_{t_1}^t a\langle\tau\rangle d\tau\right), \tag{3.19}$$

so that

$$l_\theta \sim l_{\theta 1} \exp\left(-U_1 \int_{t_1}^t a\langle\tau\rangle d\tau\right).$$

This result is the same as that of the self-preserving analysis, i.e. (3.5) and (3.6).

Another interesting comparison with the self-preserving solution can be made when the straining is *large* and *positive*. Then (3.18) shows that, when $aU_1 t \gg 1$,

$$\sigma^2 \propto \overline{v^2\langle t\rangle}/a^2 U_1^2 \quad \text{as} \quad aU_1 \tau_L \to \infty. \tag{3.20}$$

Since a strong contraction in the y direction and a divergence in the z direction lead to amplification of $\overline{v^2}$, this means that l_θ increases with time in this limit (always assuming that $t \ll \tau_L$). This disagrees with the self-similar solution (3.6a), which has the asymptotic limit that l_θ tends to a constant (K/a^*). This is more likely to be the correct limit when $t \gg \tau_L$.

Consider the thermal layer with *small* strains. It follows from (3.17) that the distortion

$$\overline{(Y - \bar{Y})\frac{d}{dt}(Y - \bar{Y})} = \frac{1}{2}\frac{d\sigma^2}{dt} = \exp\left(-A\langle t\rangle U_1\right) \int_0^t \exp\left(A\langle\tau\rangle U_1\right) \overline{v\langle t\rangle v\langle\tau\rangle}\, d\tau - aU_1 \overline{(Y - \bar{Y})^2}. \tag{3.21}$$

Thus at the beginning of the distortion ($t = t_1$)

$$\tfrac{1}{2} d\sigma^2/dt = \overline{v^2} t_1 - aU_1 \sigma^2(x = x_1),$$

where

$$\sigma^2(x = x_1) = \overline{v^2} t_1^2.$$

Therefore if the convergence is weak enough that

$$\sigma_1 a U_1/(\overline{v^2})^{\frac{1}{2}} < 1 \quad \text{or} \quad \Sigma \leqslant 1, \tag{3.22}$$

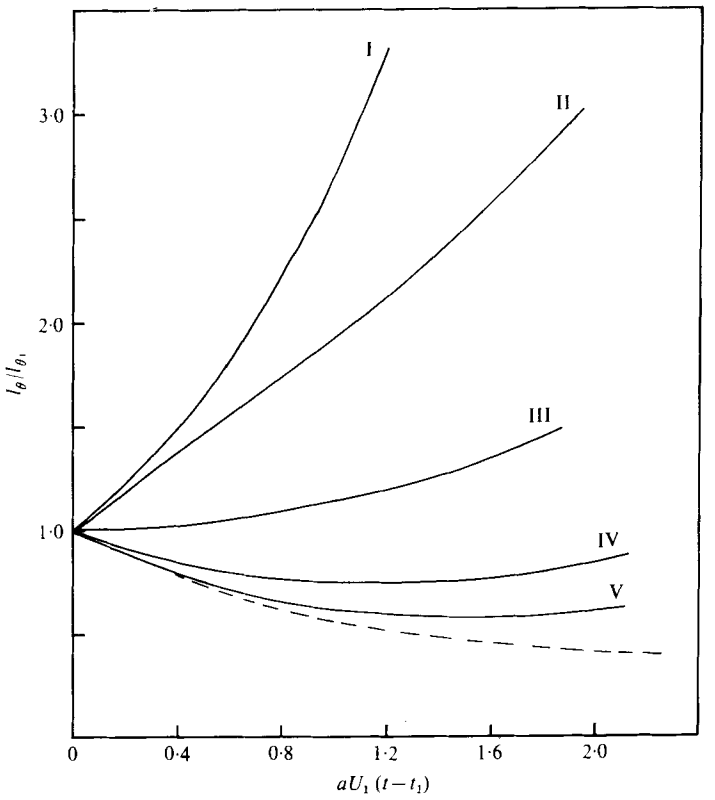

FIGURE 8. The calculated widths of thermal layers in a distorting duct, either diverging or converging, with various strengths of convergence and/or turbulence intensity, as defined by Σ. I, $\Sigma = 1{\cdot}25$, $a < 0$; II, $\Sigma = 0{\cdot}5$, $a > 0$; III, $\Sigma = 1{\cdot}0$, $a > 0$; IV, $\Sigma = 2{\cdot}0$, $a > 0$; V, $\Sigma = 3{\cdot}0$, $a > 0$. ---, asymptotic thickness of the thermal layer as predicted by a self-preserving solution.

then the widening of the thermal layer produced by the turbulence overcomes the tendency of the converging streamlines to reduce the thickness. The assumption of the self-preserving solution is that the latter effect is the stronger. So a necessary condition for the self-preserving solution to hold is the converse of (3.22), i.e. $\Sigma > 1$.

The general results of this analysis are demonstrated in figure 8 in form of a graph of $l_\theta/l_{\theta 1}$ as a function of $(t-t_1)|a|\,U_1$. Note in figure 8 how when $\Sigma = 3{\cdot}0$ the thickness of the layer first decreases, before eventually increasing. Our asymptotic result (3.20) shows that, however large Σ is, eventually l_θ will start increasing again. Asymptotically when $\Sigma \gg 1$, this increase starts (i.e. $d\sigma^2/dt = 0$) when

$$aU_1(t-t_1) \propto \ln \Sigma. \tag{3.23}$$

4. Experimental results and discussion

Thermal mixing layer

The dimensionless distributions of mean temperature across the thermal mixing layer prior to, within and after the strain field are shown in figure 9. The data were rendered dimensionless by the local characteristic intensity and length scales. It is

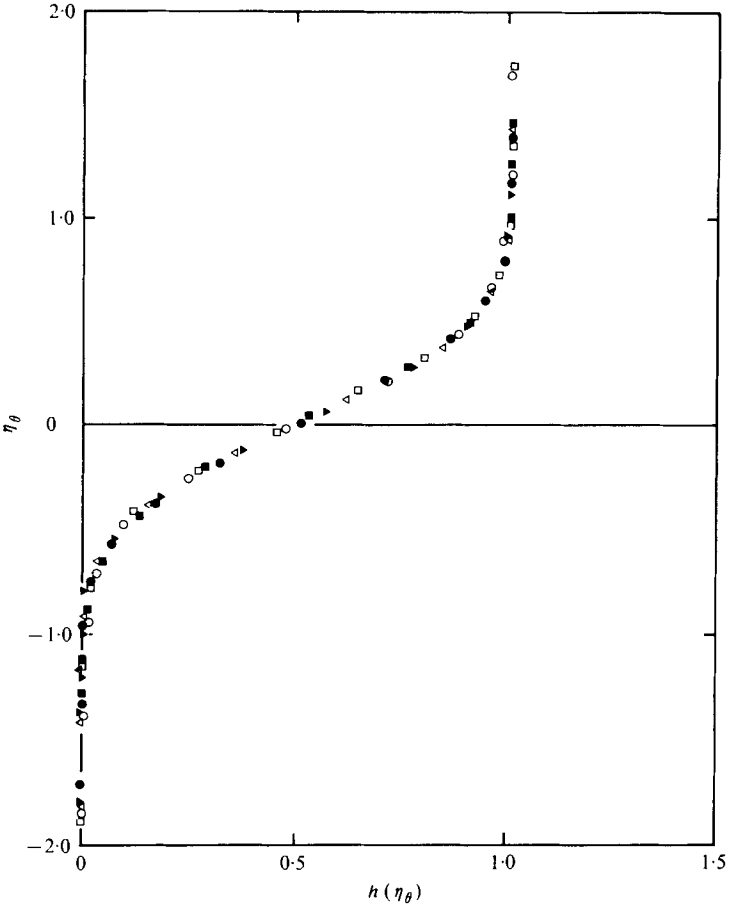

FIGURE 9. Mean temperature distributions. ○, x/M = 25; □, 50; ●, 58; ■, 74; ◁, 90; ▶, 105.

seen that there is no functional change in the mean profiles in either the uniform or the distorted region of the flow, i.e. $f(\eta)$ is a universal function.

The variation of the thermal length scale l_θ with streamwise distance is depicted in figure 10. In the pre-strain region of the flow, the measured length scale increases linearly with increasing streamwise distance, meeting the self-preserving requirements. It may be remarked that Watt (1967) and Keffer *et al.* (1977) also found, for similar experimental realizations, that l_θ increases linearly with x. The present pre-strain data are closely approximated by

$$l_\theta/M = 0{\cdot}022x/M + 1{\cdot}65. \tag{4.1}$$

From this, and using the values of x_1/M and x_2/M of 47 and 57, respectively, which were chosen on the basis of the variation of the background mean velocity U_1 along the tunnel axis (figure 2), we obtained the following predicted scales for the distorted flow:

$$l_\theta/M = \exp(-0{\cdot}01155r_1^2)\left[0{\cdot}65\int_0^{0{\cdot}034r_1}\exp(t^2)\,dt + 2{\cdot}69\right]$$

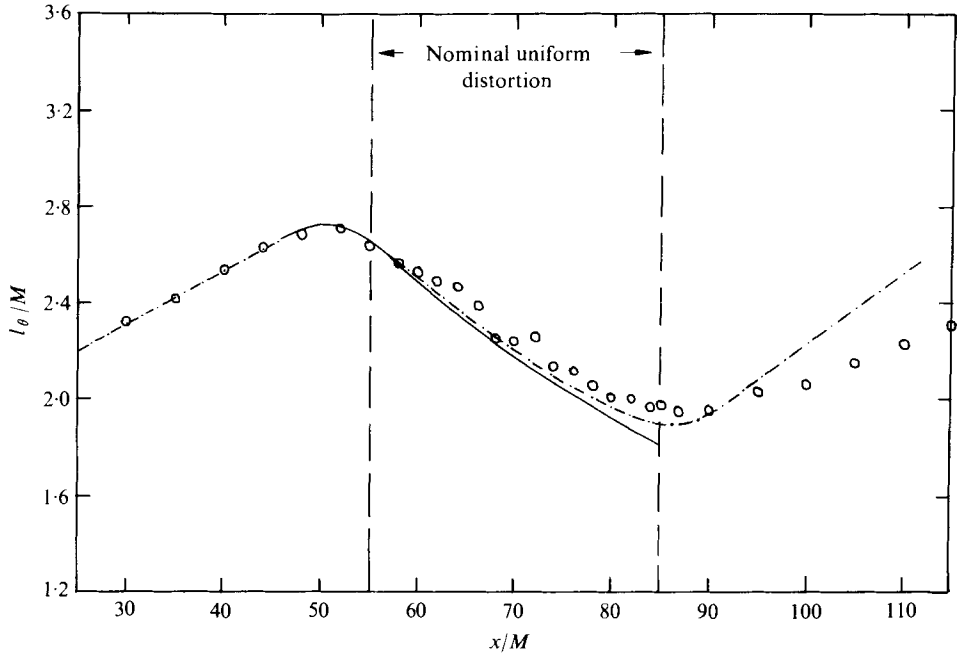

FIGURE 10. Variation of thermal length scale. ——, self-preserving solution using pre-distortion data; –·–·–·–, rapid-distortion calculation; ○–○, experiments.

for $0 \leqslant r_1 \leqslant 10{\cdot}0$ (non-uniform straining), where $r_1 = x/M - 47{\cdot}0$, and

$$l_\theta/M = 1{\cdot}643\exp(-0{\cdot}0231 r_2) + 0{\cdot}955$$

for $28{\cdot}0 > r_2 > 0$ (uniform straining), where $r_2 = x/M - 57{\cdot}0$.

As can be seen from figure 10, the behaviour of l_θ in the region of non-uniform straining is adequately modelled. The results for the region of uniform straining indicate that the width of the layer decreases, as expected from the theory, but at a rate somewhat less than that predicted, i.e. the measured scales are greater than the predicted ones throughout this region, the deviations increasing with increasing streamwise distance. It should be pointed out that the predicted curve is not applicable near the end of the distortion duct since the uniform strain field does not extend that far (see figure 2). In the post-strain region, the results show that the width of the mixing layer again increases linearly with increasing streamwise distance as expected. We note that the spreading rate in this region is slightly smaller than that in the pre-strain region.

The experimental results for the thermal length scale l_θ may also be compared with the results of the rapid-distortion analysis of § 3. First, the dimensionless temperature distribution shown in figure 9 demonstrates the self-similar form assumed in the analysis and shows that the profile is governed by the length scale l_θ. Furthermore the dimensionless profile represents accurately the error-function profile, derived by superposing a continuous distribution of point sources each of which produces a Gaussian temperature distribution.

During the pre-strain phase, assuming no dissipation in the rapid distortion of the turbulence gives

$$\overline{v\langle t_1\rangle v\langle t_2\rangle} = \overline{u_1^2},$$

so that from (3.18*b*)

$$\sigma^2(x)/M^2 = (\overline{u_1^2}/U_1^2)\,(x/M + x_0/M)^2.$$

Comparing this with (4.1) shows that $l_\theta = 2{\cdot}56\sigma(x)$.

The finite apparent scale for l_θ, at $x/M = 0$, is due to the heated grid system, and there is an effective origin for the mixing layer at $x = -x_{\theta 0}$, where in this instance $x_{\theta 0}/M = 75$. The values of $\overline{u_1^2}/U_1^2$ and of the virtual-source position derived for the initial development may be used to set the parameters in the expressions for $\sigma(x)$ and so test the theory for the later stages. Altering the value of the turbulence intensity in the pre-strain phase produces only a scaling factor in the result for l_θ. Varying the virtual-source position alters the distance over which the turbulence statistics remain well correlated, since without dissipation or straining rapid-distortion theory does not allow for any decorrelation. The effect of the straining motion is generally to increase the intensity $\overline{v^2}$, but the convergence of mean-flow streamlines acts as a decorrelating agent giving more weight to the recent history of the turbulence. So moving the virtual source back enhances the effect of streamline convergence.

The values of l_θ predicted by the rapid-distortion analysis using the pre-strain data are shown in figure 10. Allowance has been made for non-uniform straining initially, as noted previously, and the values of l_θ in the post-strain region have been calculated on the basis that the large eddies retain their overall strain after leaving the straining section. The results based on rapid-distortion theory are in good agreement with the observations, and also illustrate the recovery of the diffusion process after the flow leaves the straining section. However during the straining l_θ is underestimated slightly and, in the post-strain region, its predicted growth is too rapid. The latter is due to an overestimate of the intensity $\overline{v^2}$ by rapid-distortion theory. During the straining, the value of $\overline{v^2}$ is not so important, as the results are dominated by the convergence of mean-flow streamlines, which produces the reduction in l_θ. But this is no longer so in the post-strain region, and the increased value of $\overline{v^2}$ is important.

Note that for these experiments the parameter Σ, which is a measure of the importance of straining relative to turbulent diffusion, is given by

$$\Sigma = \frac{l_\theta(x = x_1)\,aU_1}{u_1'} = \frac{2{\cdot}8 \times 0{\cdot}0254 \times 0{\cdot}9}{0{\cdot}02} \simeq 3{\cdot}2.$$

Therefore $\Sigma > 1$ and the straining dominates, which is why the self-preserving solution proves reasonably satisfactory. We also note that the time $t_2 - t_1$ required to pass through the distortion region is such that $(t_2 - t_1)\,aU_1 = 0{\cdot}254 \times 30 \times 0{\cdot}9 \doteq 0{\cdot}7$, so that $(t_2 - t_1)\,aU_1 < 1{\cdot}6$, which is a necessary condition for dl_θ/dx to be negative in the contraction (see §3 and figure 8).

It is interesting that the thermal field responds so quickly after being released from the strain field. Measurements by Grant (1958) on a uniformly strained, grid-generated turbulent field suggested that the time scale for the recovery of the turbulence was of the same order as the characteristic decay time for the intensity fluctuations and consequently the approach to pre-strain isotropy was slow. It can be seen from figure 11,

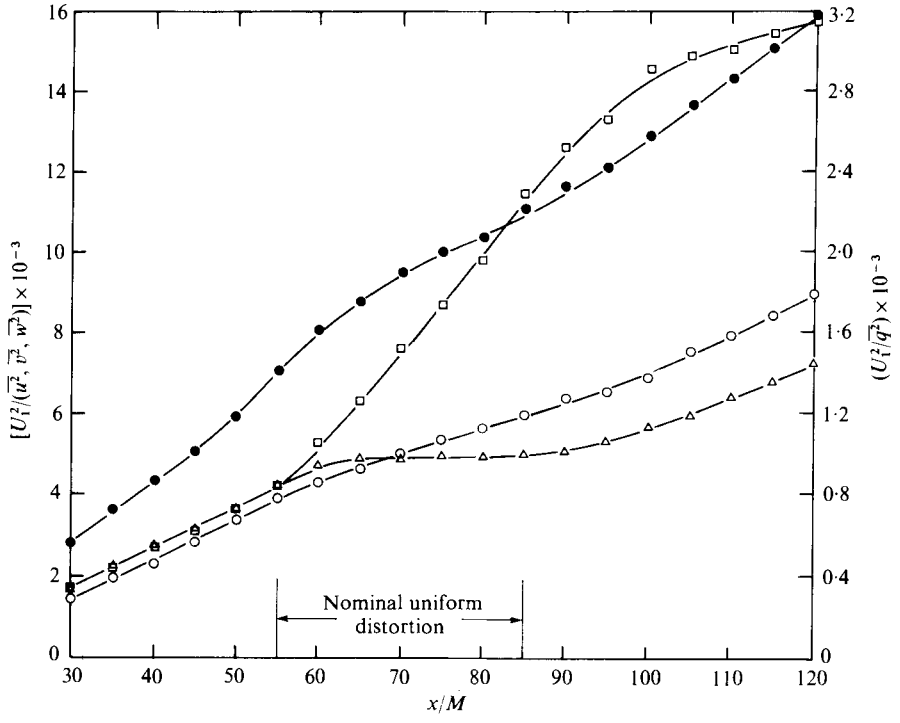

FIGURE 11. Variation of turbulence intensities. ○, U^2/u^2; △, U^2/v^2; □, U^2/w^2; ●, U^2/q^2.

which shows the variation of the turbulence intensities of the convecting flow along the centre-line of the tunnel, plotted as inverse ratios $U_1^2/\overline{u^2}$ etc., that this is also the case in the present situation. It may be remarked that Tucker & Reynolds (1968) found that their flow field rapidly became less anisotropic upon being released from the strain field. The reason for this rather different response is unexplained.

As can be seen from figure 11, the component of intensity $\overline{v^2}$ increases slightly with straining and its overall decay is less than that of the other components. Physically this is due to the stretching of vortex line elements in the z direction; and the reduction in $\overline{w^2}$ is caused by the contraction of elements in the y direction. A comparison of these results with the predictions of $\overline{v^2}$ from rapid-distortion theory is given in figure 12. One estimate with no dissipation, as given by Batchelor & Proudman (1954), and one with an overall decay factor, as suggested by Ribner & Tucker (1952), are included.

The decay factor, based on initial data and the intensities at $x/M = 40$ given in table 1, is assumed to be

$$\overline{v^2}/U_1^2 = 100(x/M - 13)^{-1}\,[\overline{v^2}/U_1^2],$$

where $[\overline{v^2}/U_1^2]_0$ is the calculated intensity without decay. Even so we find that the value of $\overline{v^2}/U_1^2$ is too large. The rapid distortion produces components with large wave-number, which are no longer within the range of the energy-containing eddies and would be dissipated rapidly. The lack of viscous decay and inertial transfer in the theory means that the anisotropy produced is overestimated.

The ability of the rapid-distortion approach to give the behaviour of the thermal mixing layer itself poses some questions, since $u'/(aU_1 L_x) \sim 1{\cdot}4$ and $l_\theta/L_x \sim 1{\cdot}5$,

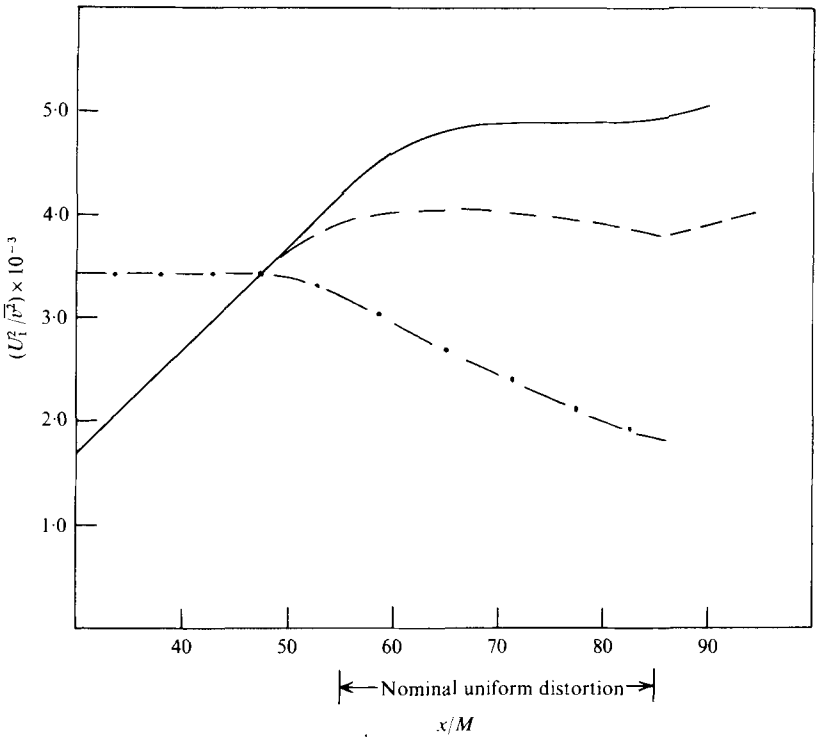

FIGURE 12. Comparison of calculations and observations of the distortion of the component $\overline{v^2}$ of turbulence intensity. ——, observations; – – –, rapid distortion with decay; –·–·–, rapid distortion without decay.

which satisfy neither $u'/(aU_1 L_x) \ll 1$ nor $l_\theta/L_x \ll 1$. Also the initial growth of l_θ is linear with distance downstream, consistent with short-time-scale diffusion in a field of constant intensity, whilst from figure 12 it can be seen that the total turbulent intensity is decaying appreciably. From the linear growth of l_θ an effective turbulent intensity may be estimated:

$$\overline{(u_{10}^2}/U_1^2)_{\text{eff}}^{\frac{1}{2}} = 0{\cdot}0086,$$

which, compared with the intensity at $x/M = 40$ of 0·0202, shows that only 15 % of the total turbulent energy is effective in this diffusion process. This suggests that diffusion in this case is governed by large permanent eddies of the type discussed by Batchelor (1953, p. 80), which remain well-correlated motions for a long time. These would in turn be strongly influenced by the method of generation of the turbulence at the grid. It would appear that the processes of turbulence generation and marking of the flow by heating at the grid are very complicated.

Velocity mixing layer

The dimensionless measured velocity profiles in the velocity mixing layer are plotted in figure 13. A comparison of figures 9 and 13 shows that $f(\eta) = h(\eta_\theta)$. This is not surprising since these functions satisfy formally identical equations and have the same boundary conditions. The variation of the velocity length scale l_0 with streamwise

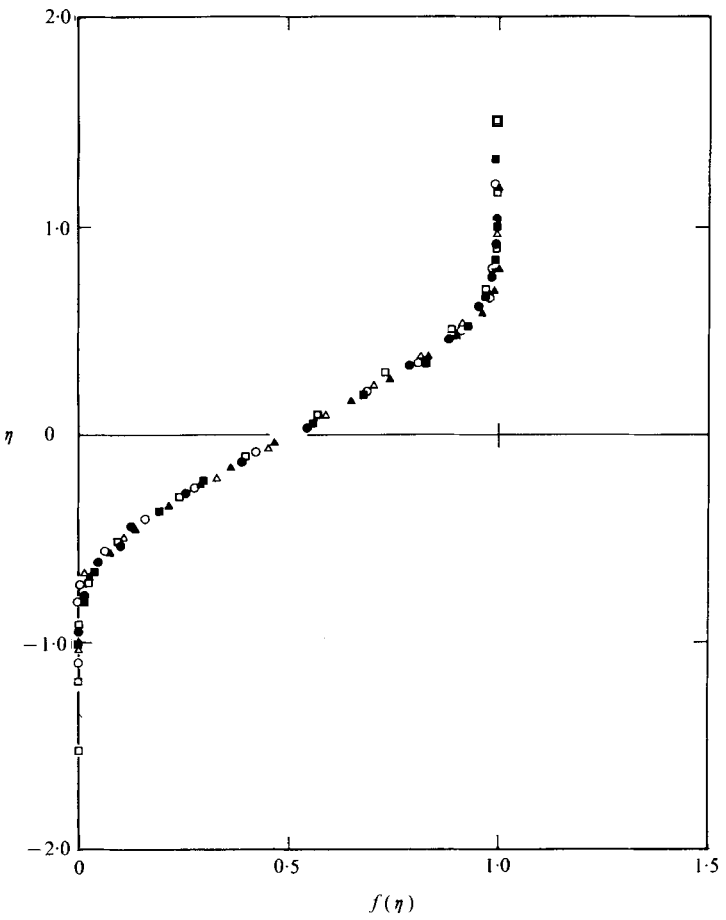

FIGURE 13. Mean velocity distributions. □, $x/M = 30$; ○, 45; △, 60; ■, 75; ●, 90; ▲, 105.

distance is presented in figure 14. Within the pre-strain region, l_0, like l_θ, increases linearly with increasing streamwise distance, as predicted. It is noted that a linear behaviour of l_0 in an unstrained region was also found by Watt (1967) and by Wygnanski & Fiedler (1970). The present pre-strain data conform to the relation

$$l_0/M = 0{\cdot}040x/M + 0{\cdot}80,$$

from which the predicted scales in the strained regions were found to be

$$l_0/M = \exp(-0{\cdot}001155r_1^2)\left[1{\cdot}177\int_0^{0{\cdot}034r_1}\exp(t^2)\,dt + 2{\cdot}68\right]$$

for $0{\cdot}0 \leqslant r_1 \leqslant 10{\cdot}0$ (non-uniform straining) and

$$l_0/M = 1{\cdot}031\exp(-0{\cdot}0231r_2) + 1{\cdot}732,$$

for $28{\cdot}0 \geqslant r_2 \geqslant 0{\cdot}0$ (uniform straining).

Again, as in the case of the thermal mixing layer, the measured scales are well approximated by the values predicted by theory based on self-preserving profiles for the non-uniformly strained region; they are somewhat larger than the values predicted

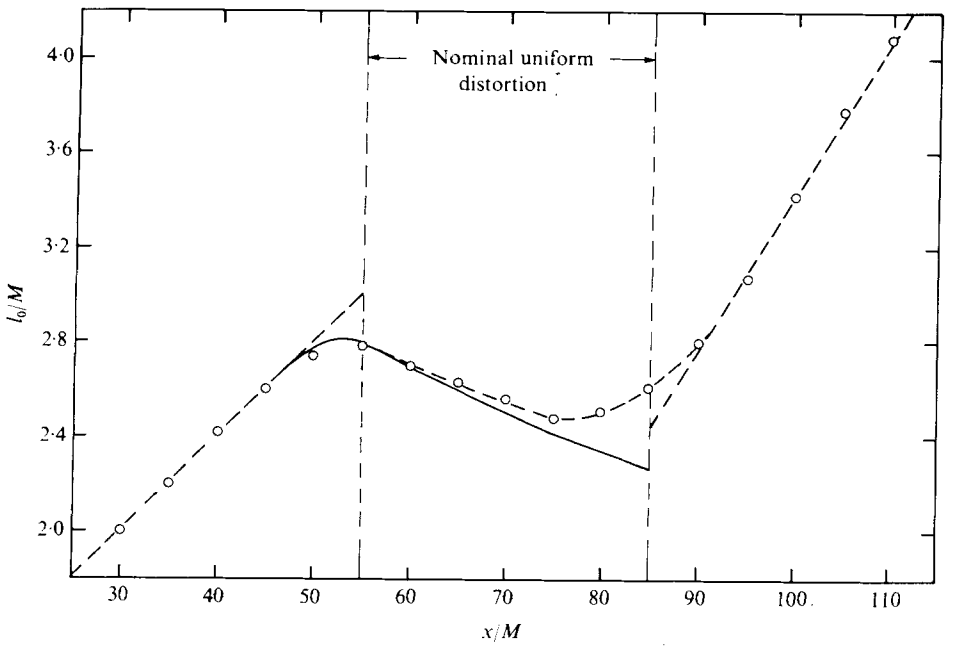

FIGURE 14. Variation of velocity length scales. ——, self-preserving solution using pre-distortion data.

within the uniform strain field and they display a linear behaviour in the post-strain region in accordance with the self-preserving theory. Unlike the thermal mixing layer, however, the velocity mixing layer expands at a noticeably *greater* rate in the post-strain region than it does in the pre-strain region.

The departure of l_0 from the predicted self-preserving form within the uniform-straining region is attributed also to the effect of the strain field on the turbulence. The lateral momentum transport term $\overline{uv}$, upon whose behaviour l_0 depends, will respond to the strain in much the same manner as $\overline{v\theta}$, so that, in view of the behaviour of the components $\overline{u^2}$ and $\overline{v^2}$ of the grid turbulence within the distortion (figure 12), we should expect l_0 to be slightly larger than is predicted. This is consistent with the experiments carried out on the strained wake (Keffer 1965), which demonstrated that the existence of self-preserving solutions to the equations of motion is not a sufficient condition for realization in practice.†

From a comparison of figures 10 and 14, it can be seen that the spreading rate of the unstrained velocity mixing layer is roughly 80 % greater than that of the corresponding thermal layer, whereas for the uniformly strained flows, the spreading rate of the thermal layer is about 65 % greater than that of the velocity layer. This is consistent with the fact that turbulent diffusion will be significantly greater in a flow having large lateral gradients of streamwise mean velocity (i.e. large mean-flow shear) than in a grid-generated turbulent flow. (Typically the turbulence intensities are in the ratio 0·1 to 0·02.)

We note that, for a combined thermal–velocity mixing layer, the widths of the

† Further measurements and a comparison of the measurements with rapid-distortion theory have recently been completed by Elliott (1976).

thermal and velocity fields should be identical at all streamwise locations, as has been found for the heated two-dimensional turbulent jet by Davies, Keffer & Baines (1975).

The authors would like to thank R. G. Blumenauer, who caried out the experiments on the thermal mixing layer. This research was supported by the National Research Council of Canada under Grant number A-2746. M. Maxey acknowledges the support of a Science Research Council postgraduate studentship.

Appendix A. Self-preserving solutions

In the experimental modelling of a uniformly strained mixing layer, it is not possible to initiate the strain field instantaneously. In the analysis which follows, we therefore assume that a gradual straining begins at $x_1 < x_c$ (x_c being the nominal distance to the start of the distortion duct) and extends to $x_2 > x_c$, and that uniform straining is initiated at x_2. Furthermore, we assume that the mixing layer is in a self-preserving state before it is strained.

The equation of mean motion for the steady incompressible flow of a velocity mixing layer along the central plane of a distortion duct can be approximated as

$$\overline{U}\frac{\partial \overline{U}}{\partial x} + \overline{V}\frac{\partial \overline{U}}{\partial y} + \frac{\partial \overline{uv}}{\partial y} = 0,$$

where viscous and normal-stress terms, being of second order, are ignored and

$$V = -\frac{dS}{dx}(x)\, y\overline{U}.$$

$S(x)$ is a strain function such that

$$S(x)\begin{cases} = 0 & \text{for} \quad x \leqslant x_1, \\ > 0 & \text{for} \quad x_2 > x > x_1, \\ = a(x-x^*) & \text{for} \quad x > x_2, \end{cases}$$

where a is the strain constant for uniform straining and $x^* = \frac{1}{2}(x+x_2)$. Following Reynolds (1962), we assume a parabolic variation for $S(x)$ in the region $x_2 > x > x_1$, i.e.

$$S(x) = A(x-B)^2.$$

Since the variation of $S(x)$ is continuous, it follows that $A = a/2(x_2-x_1)$ and $B = x_1$, so that

$$S(x) = a(x-x_1)^2/2(x_2-x_1) \quad \text{for} \quad x_2 > x > x_1. \tag{A 1}$$

We introduce universal functions $f(\eta)$ and $g(\eta)$ as follows:

$$\overline{U} = U_2 + u_0(x) f(\eta) \tag{A 2}$$

and

$$\overline{uv} = u_0^2(x)\, g(\eta), \tag{A 3}$$

where u_0 is the characteristic intensity scale of the flow and $\eta \equiv (y-y_{0\cdot5})/l_0(x)$ is the dimensionless lateral co-ordinate, $y_{0\cdot5}$ being the lateral distance between the maximum and half-maximum mean velocity points and l_0 the characteritic length scale of the flow. l_0 is taken to be the lateral distance between the 90 and 10 % maximum mean

velocity points, i.e. $l_0 = y_{0.9} - y_{0.1}$. Substitution of (A 2) and (A 3) into the governing equation yields

$$\left[\frac{U_2}{u_0}+f\right]\left[\frac{l_0}{u_0}\frac{du_0}{dx}f-\left\{\frac{dl_0}{dx}+\frac{dS}{dx}l_0\right\}\eta f'\right]+g' = 0, \tag{A 4}$$

where the prime denotes differentiation with respect to η. Self-preservation requires that the coefficients of the universal functions and their derivatives be constant or zero. Thus

$$u_0 = \text{constant} \tag{A 5}$$

and

$$\frac{dl_0}{dx}+\frac{dS}{dx}l_0 = \text{constant} = C_1. \tag{A 6}$$

It is convenient to equate u_0 to the velocity difference between the free streams of the mixing layer, i.e. $u_0 = U_1 - U_2$. Solving (A 6) in the region $x_2 > x > x_1$ gives

$$l_0 = l_{01} = C_1 \exp[-S(x)]\left[\int_{x_1}^{x} \exp[S(x')]\,dx' + C_2\right]. \tag{A 7}$$

Since $l_0(x)$ is continuous at x_1

$$l_{01}(x_1) = l_0^*(x_1), \quad \text{where} \quad l_0^* = C(x-x_0),$$

which is the characteristic length scale for the undistorted flow. C and x_0 are constants. Consequently $C_2 = (C/C_1)(x_1 - x_0)$, and substituting (A 1) into (A 7) yields

$$l_{01} = C_1 \exp(-ar^2/2r_0)\left\{\left(\frac{2r_0}{a}\right)^{\frac{1}{2}}\int_0^{r(a/2r_0)^{\frac{1}{2}}} \exp(t^2)\,dt + \frac{C}{C_1}(x_1 - x_0)\right\}, \tag{A 8}$$

where $r = x - x_1$ and $r_0 = x_2 - x_1$. Also, l_{01} must satisfy the following condition:

$$\lim_{a\to 0} l_{01} = l_0^*,$$

whence $C_1 = C$.

In the region $x > x_2$, we obtain from (A 6)

$$l_0 = l_{02} = C_1' \exp[-S(x)]\left[\int_{x_2}^{x} \exp[S(x')]\,dx' + C_2'\right], \tag{A 9}$$

$$l_{02}(x = x_L) = l_{01}(x = x_L),$$

so that from (A 8) and (A 9), since $l_0(x)$ is continuous at $x = x_L$,

$$C_1' C_2' \exp[-a(x_2 - x^*)] = CC_{01},$$

where

$$C_0 = \exp(-\tfrac{1}{2}ar_0)\left[\left(\frac{2r_0}{a}\right)^{\frac{1}{2}}\int_0^{(\frac{1}{2}ar_0)^{\frac{1}{2}}} \exp(t^2)\,dt + x_1 - x_0\right] = \text{constant} \quad (a \neq 0).$$

Hence

$$l_{02} = C' a^{-1}\{1 - \exp[-a(x-x_2)]\} + CC_0 \exp[-a(x-x_2)].$$

Since l_{02} must satisfy the condition $\lim_{a\to 0} l_{02} = l_0^*$, we find $C' = C$. Thus, for $x > x_2$,

$$l_0 = Ca^{-1}\{1 + (aC_0 - 1)\exp[-a(x-x_2)]\}. \tag{A 10}$$

It should be noted that the constants in (A 10) can be determined once l_0^* is known.

For the thermal mixing layer, we follow a development parallel to that for the velocity mixing layer. The general two-dimensional heat-transfer equation, when molecular conduction and streamwise variation of the longitudinal heat-transport term are negligible, is

$$\bar{U}\frac{\partial\Theta}{\partial x}+\bar{V}\frac{\partial\Theta}{\partial y}+\frac{\partial\overline{v\theta}}{\partial y}=0. \tag{A 11}$$

Along the central plane of a distorting duct, and in the absence of a velocity shear flow, this takes the special form

$$U_1\left[\frac{\partial\Theta}{\partial x}-\frac{\partial S}{dx}y\frac{\partial\Theta}{\partial y}\right]+\frac{\partial\overline{v\theta}}{\partial y}=0, \tag{A 12}$$

where U_1 is the mean velocity of the convecting flow and is constant. We introduce universal functions $h(\eta_\theta)$ and $j(\eta_\theta)$ corresponding to (A 2) and (A 3):

$$\Theta=\theta_0 h(\eta_\theta) \tag{A 13}$$

and

$$\overline{v\theta}=u_0\theta_0 j(\eta_\theta), \tag{A 14}$$

where θ_0 is the characteristic thermal intensity scale, $\eta_\theta\equiv(y-y_{0\cdot5})/l_\theta(x)$ is the thermal equivalent of η, l_θ being the characteristic thermal length scale for the flow, and u_0 is the characteristic velocity intensity scale, which is taken as constant (and can be taken as U_1). This implies small variations in $\overline{v\theta}$ and a strong contraction. In view of the boundary condition

$$\Theta(x,y=\infty)=\Theta_m=\text{constant},$$

where Θ_m is the maximum (mean) temperature difference across the flow, it follows that $\theta_0=$ constant. Here we take θ_0 to be equal to Θ_m. Substitution of (A 13) and (A 14) into (A 12) gives

$$U_1\left[\frac{\partial}{\partial x}(\theta_0 h)-\frac{dS}{dx}\eta_\theta l_\theta\frac{\partial}{\partial y}(\theta_0 h)\right]+\frac{\partial}{\partial y}(u_0\Theta_{0j})=0. \tag{A 15}$$

This reduces to

$$-\frac{U_1}{u_0}\left[\frac{dl_\theta}{dx}+\frac{dS}{dx}l_\theta\right]\eta_\theta h'+j'=0. \tag{A 16}$$

For self-preservation of the flow to be possible, it is necessary that

$$\frac{dl_\theta}{dx}+\frac{dS}{dx}l_\theta=\text{constant}=K_1, \tag{A 17}$$

from which, in the region $x_2>x>x_1$,

$$l_\theta=l_{\theta1}=K_1\exp[-S(x)]\left[\int_{x_1}^{x}\exp[S(x')]\,dx'+K_2\right].$$

Application of the condition $l_{\theta1}|_{x=x_1}=l_0^*|_{x=x_1}$, where $l_\theta^*=K(x-x_{\theta0})$, which is the characteristic thermal length scale for the undistorted mixing layer and in which K and $x_{\theta0}$ are constants, gives

$$K_2=(K/K_1)(x_1-x_{\theta0}).$$

Also, application of the condition $\lim_{a\to 0} l_{\theta 1} = l_\theta^*$ gives $K_1 = K$. Thus for $x_2 > x > x_1$, using (A 1),

$$l_\theta = K\exp(-ar^2/2r_0)\left\{\left(\frac{2r_0}{a}\right)^{\frac{1}{2}}\int_0^{r(a/2r_0)^{\frac{1}{2}}}\exp(t^2)\,dt + (x_1 - x_{\theta 0})\right\}. \tag{A 18}$$

Similarly, for the region $x > x_2$, we obtain from (A 17)

$$l_\theta = Ka^{-1}\{1 + (aK_0 - 1)\exp[-a(x - x_2)]\}, \tag{A 19}$$

where

$$K_0 = \exp(-\tfrac{1}{2}ar_0)\left[(2r_0/a)^{\frac{1}{2}}\int_0^{(\frac{1}{2}ar_0)^{\frac{1}{2}}}\exp(t^2)\,dt + (x_1 - x_{\theta 0})\right] = \text{constant} \quad (a \neq 0).$$

Appendix B. Homogeneous rapid distortion

The method of rapid strain distortion and the assumptions involved are summarized by Townsend (1976, § 3.10). The nonlinear terms and the viscous terms in the equations for the fluctuating velocities are neglected, on the assumption that

$$u'/(aU_1 L_x) \ll 1 \quad \text{and} \quad \nu/(aU_1 L_x^2) \ll 1,$$

where ν is the kinematic viscosity. From the values of the turbulent intensity at $x/M = 40$, given in table 1, $u'/(aU_1 L_x) \sim 1{\cdot}4$ and $\nu/(aU_1 L_x^2) \sim 1{\cdot}7 \times 10^{-3}$. The neglect of the nonlinear terms is thus not strictly justified. The reduced equations are

$$\partial u_i/\partial t + U_j\,\partial u_i/\partial x_j + u_j\,\partial U_i/\partial x_j = -\partial p/\partial x_i,$$
$$\partial u_i/\partial x_i = 0,$$

where p is the kinematic pressure, i.e. pressure divided by density.

The effect of mean-flow convection is accounted for by a change of co-ordinates, defined by

$$X = x - U_1 t, \quad Y = y\exp(A(t)\,U_1), \quad Z = z\exp(-A(t)\,U_1),$$

where $A(t) = S(x)/U$, and by the usual total strains, which in this case are

$$e_1 = 1, \quad e_2 = \exp(-A(t)\,U_1), \quad e_3 = \exp(A(t)\,U_1).$$

The resulting vorticity fluctuations are then given by

$$\omega_i(X, Y, Z, t) = e_i\,\omega_i(X, Y, Z, 0), \quad i = 1, 2, 3.$$

Fourier components of the velocity fluctuations in the new co-ordinate system may be defined in terms of distributions or generalized functions, with

$$u_i(\mathbf{X}, t) = \int \exp(i\,\mathbf{k}.\mathbf{x})\,a_i(\mathbf{k}, t)\,d^3\mathbf{k},$$

where the $a_i(K, t)$ are the Fourier components, $\mathbf{k}$ being the wavenumber vector. These components are distorted by the straining motion:

$$a_1(\mathbf{k}, t) = \chi^{-2}\{(k_2^2 e_3/e_2 + k_3^2 e_2/e_3)\,a_1(\mathbf{k}, 0) + [-(e_3/e_2)\,k_1 k_2]\,a_2(\mathbf{k}, 0) + (-(e_2/e_3)\,k_1 k_3)\,a_3(\mathbf{k}, 0)\},$$

where

$$\chi^2(t) = (k_1^2/e_1^2 + k_2^2/e_2^2 + k_3^2/e_3^2),$$

with similar expressions for a_2 and a_3. These may be summarized as

$$a_i(\mathbf{k}, t) = A_{ij}(\mathbf{k}, t)\,a_j(\mathbf{k}, 0).$$

As the turbulence is homogeneous, the power spectrum

$$\Phi_{ij}(\mathbf{k},\, t)\, \delta(\mathbf{k}-\mathbf{k}') = \overline{a_i^*(\mathbf{k},t)\, a_j(\mathbf{k}',t)},$$

where the asterisk denotes the complex conjugate. In particular, it is assumed that, in unstrained conditions, the turbulence is isotropic, with

$$\Phi_{ij}(\mathbf{k}, 0) = (k_i k_j - k^2\delta_{ij})\, \psi(k),$$

and that, at this initial instant, the wavenumber vectors are the same in both co-ordinate systems. On the basis of these assumptions space–time correlations may be derived and the velocity correlation in the frame moving along mean-flow streamlines is

$$\begin{aligned}\overline{v\langle t_1\rangle v\langle t_2\rangle} &= \int A_{2i}(\mathbf{k}, t_1)\, A_{ij}(\mathbf{k}, t_2)\, (k_i k_j - k^2\delta_{ij})\, \psi(k)\, d^3\mathbf{k} \\ &= \frac{\overline{3u_{10}^2}}{8\pi}\int_0^{2\pi} d\phi \int_0^{\pi} d\theta \sin\theta \{A_{21}(\theta,\phi,t_1)\, A_{ij}(\theta,\phi,t_2)(-k_i k_j/k^2 + \delta_{ij})\},\end{aligned}$$

where (θ, ϕ) are polar co-ordinates of $\mathbf{k}$, i.e. $k_1 = k\sin\theta\cos\phi$, $k_2 = k\sin\theta\sin\phi$ and $k_3 = k\cos\theta$, and the operators $A_{ij}(\mathbf{k}, t)$ depend only on (θ, ϕ, t) and not on k. This result is independent of the initial form of the energy spectrum, $\overline{(u_{10}^2)^{\frac{1}{2}}}$ being the initial intensity. These integrals have been evaluated by numerical integration, and intensities and diffusive spreads derived. The expression for the variance of particle position may be rewritten as

$$\frac{\sigma(x/M)^2}{M^2} = \frac{3}{8\pi}\frac{\overline{u_{10}^2}}{\overline{U_1^2}}\int_0^{2\pi} d\phi \int_0^{\pi} d\theta \sin\theta \left\{B_{2i}\left(\theta,\phi,\frac{x}{M}\right) B_{2j}\left(\theta,\phi,\frac{x}{M}\right)(\delta_{ij} - k_i k_j/k^2)\right\}, \tag{B 1}$$

$$B_{ij}\left(\theta,\phi,\frac{x}{M}\right) = \int_0^{x/M} A_{ij}(\theta,\phi,t = x_1/U_1)\exp\{-(S(x) - S(x_1))\}\, d(x_1/M),$$

with e_2 and e_3 given as functions of position x/M.

The values of l_θ plotted in figure 10 were computed from (A 20), using the scaling factor $l_\theta = 2{\cdot}56\sigma$ mentioned in § 4.

REFERENCES

Batchelor, G. K. 1953 *The Theory of Homogeneous Turbulence.* Cambridge University Press.

Batchelor, G. K. & Proudman, I. 1954 *Quart. J. Mech. Appl. Math.* **7**, 83.

Batchelor, G. K. & Townsend, A. A. 1956 Turbulent diffusion. In *Surveys in Mechanics* (ed. G. K. Batchelor & R. M. Davis), p. 352. Cambridge University Press.

Britter, R. E., Hunt, J. C. R. & Puttock, J. S. 1976 *Proc. Conf. Systems and Models in Air and Water Pollution.* London: Inst. Measurement and Control.

Comte-Bellot, G. & Corrsin, S. 1971 *J. Fluid Mech.* **48**, 273.

Davies, A. E., Keffer, J. F. & Baines, W. D. 1975 *Phys. Fluids* **17**, 770.

Elliott, C. J. 1976 Ph.D. thesis, University of Cambridge.

Grant, H. L. 1958 *J. Fluid Mech.* **4**, 149.

Grant, H. L. & Nisbet, I. C. T. 1957 *J. Fluid Mech.* **2**, 263.

Hunt, J. C. R. 1973 *J. Fluid Mech.* **61**, 625.

Hunt, J. C. R. & Mulhearn, P. J. 1973 *J. Fluid Mech.* **61**, 245.

Keffer, J. F. 1965 *J. Fluid Mech.* **22**, 135.

Keffer, J. F. 1967 *J. Fluid Mech.* **28**, 183.

KEFFER, J. F., OLSEN, G. J. & KAWALL, J. G. 1977 *J. Fluid Mech.* **79**, 595.

MARÉCHAL, J. 1972 *J. Méc.* **11**, 18.

MILLS, R. R. & CORRSIN, S. 1959 *N.A.S.A. Memo.* no. 5-5-59 W.

MONIN, A. S. & YAGLOM, A. M. 1971 *Statistical Fluid Mechanics.* M.I.T. Press.

PORTFORS, E. A. 1969 Ph.D. thesis, University of Toronto.

REYNOLDS, A. J. 1962 *J. Fluid Mech.* **13**, 333.

RIBNER, H. S. & TUCKER, M. 1952 *N.A.C.A. Tech. Note* no. 2606.

TOWNSEND, A. A. 1954 *Quart. J. Mech. Appl. Math.* **7**, 104.

TOWNSEND, A. A. 1976 *The Structure of Turbulent Shear Flow*, 2nd edn. Cambridge University Press.

TUCKER, H. J. & REYNOLDS, A. J. 1968 *J. Fluid Mech.* **32**, 657.

VAN ATTA, C. W. & CHEN, W. Y. 1969 *J. Fluid Mech.* **38**, 743.

WATT, W. E. 1967 Ph.D. thesis, University of Toronto.

WYGNANSKI, I. & FIEDLER, H. 1970 *J. Fluid Mech.* **41**, 327.